Traveltime Residual Estimation for some Seismic Stations within Southeast Asia using a New Ray Tracing Algorithm

Abel Uyimwen Osagie[1] and Oke Israel Okwokwo[1,2]

[1] *University of Abuja, Nigeria.*
[2] *University of Manchester, UK.*
Corresponding author: Abel U. Osagie abel.osagie@uniabuja.edu.ng

Abstract
Path dependent corrections relative to traveltimes have been demonstrated to improve event locations. Using available global velocity models, direction-based station corrections can be estimated in a region without calibration data. In this study, traveltime corrections have been obtained for 113 broadband seismic stations within southern Thailand, Peninsular Malaysia, Singapore and Sumatra region of Indonesia. A total of 97,124 first-arrival p-waves are obtained from 15,180 earthquakes that have occurred around the Sumatra Subduction Zone between 1964 and 2018. The dataset is a combination of arrival times from the bulletin of International Seismological Centre and waveforms from the Incorporated Research Institutions for Seismology. A new algorithm for three-dimensional ray tracing is used to compute traveltimes and raypaths. The corrections are based on the ak135 velocity models at four back-azimuthal directions. Stations with 100 or more arrivals are selected in this study. Station KULM in Peninsular Malaysia recorded the highest number with 5425 arrivals. The estimated residuals range from -0.02 to 0.76 seconds (s) for stations distributed around southern Thailand and a range of 0.48 to 1.09 s for stations within Peninsular Malaysia. A range of 0.37 to 0.54 s for stations within Singapore and -0.55 to 2.04 s for stations distributed around Sumatra (in Indonesia). Stations LEM, KLM and KGM show consistent high residual values at all calculated angles and distances. The result of this study will support routine location of hypocentral parameters within the region. The scheme has been implemented in the forward computational process of a seismic tomographic inversion program.
Keywords*: Ray-tracing, Station Correction, P-wave, Southeast Asia*

I.   Introduction

Precise location of earthquakes continues to be among the main objectives of seismology. This helps to make good inference about the subsurface structures responsible for the observed seismicity. Knowledge of the subsurface brings many other benefits which may be economic or safety related (e.g., in mineral exploration or engineering designs). Unfortunately, events with smaller magnitudes at regional distances are usually recorded by fewer stations around the region. Besides, the precision of locations is affected by limitations imposed by other factors like data quality, the velocity model and the algorithm used for locating the events. There are usually tradeoffs between earthquake locations and velocity model. Fortunately, technological advances have improved the quality of seismic data and different algorithms have been developed to increase the reliability of event locations. However, information about near-surface velocity structures at local/regional distances is not common knowledge in many regions.

Global one-dimensional (1D) reference velocity models like PREM (Dziewonski and Anderson, 1981), iasp91 (Kennett and Engdahl, 1991) and ak135 (Kennett *et al.,* 1995) are good approximations for the purpose of locating hypocentral parameters. However, these approximations may not satisfy velocity variations at local and regional distances. This is due to lateral variations in the crustal and upper mantle which cause deviations in predicted raypaths. The raypath deviation can introduce errors in traveltime calculations. The Group of Scientific Experts' Third Technical Test (GSETT3) has adopted the IASPEI91 (Kennett and Engdahl, 1991) model as the reference traveltime set since 1st January, 1995 (Yang *et al*., 2001). The IASPEI91 traveltimes can deviate considerably from true traveltimes at regional distances. The deviation in traveltime and raypath can be as much as 2 seconds and 100 km respectively (Spakman and Bijwaard 2000), and as much as 3.9 seconds and 77 km respectively (Zhao and Lei, 2004).

The effect of lateral heterogeneity can be reduced, either by, (1) using regional velocity model or by, (2) applying traveltime corrections to known models for event locations (Yang, et al., 2001). The former requires the development of improved velocity models of the crust and mantle for better prediction of seismic traveltimes (e.g., Villaseñor et al., 2003) while the latter applies traveltime corrections based on the residuals

observed for calibration events of known locations (Shearer, 2001). Station corrections e.g., the Source-Specific Station Correction (SSSC) may be required to account for the effect of lateral heterogeneity at a given seismic station. These model-predicted SSSC's may be obtained by ray tracing techniques through the model from each station to points on a specified latitude-longitude grid within specified distances from the station (Villaseñor et al., 2003). Station corrections can be constructed in regions (e.g., with frequent earthquakes and/or explosions) to obtain good calibration data. Regional SSSCs for International Monitoring System (IMS) stations have been developed. Path dependent corrections relative to the IASPEI91 traveltimes have been demonstrated to improve event locations (e.g., Yang et al., 2001). Unfortunately, many regions around the globe do not have calibration data. Hence, station correction may be estimated using available regional and/or global velocity models.

The aim of this research is to estimate the average traveltime residual values (**AR**) for some stations distributed around the southern part of Thailand, Peninsular Malaysia, Singapore and the Sumatra region of Indonesia. The **AR** will be estimated based on back-azimuth (θ) for regional first arrival p-phases at up to 1500 km epicentral distances (Δ). To achieve the aim, a new three-dimensional (3D) ray tracing algorithm is developed to compute traveltimes and raypaths at local and regional distances. The algorithm is can use any global one-dimensional (1D) velocity model as reference to create a 3D model. Calculations of traveltime residual values (**R**) for stations are based on θ within four quadrants: NE ($\theta \leq 90°$), SE ($90° < \theta \leq 180°$), SW ($180° < \theta \leq 270°$) and NW ($270° < \theta \leq 360°$) directions. The overall calculated average residual values (**AR**) are compared with the results published by the bulletin of International Seismological Center (ISC). Traveltimes computed with the scheme for hand-picked waveforms from the Incorporated Research Institutions for Seismology (IRIS) are also validated by the results obtained from the TauP Toolkit software (Crotwell et al., 1999) for the same velocity model, hypocenters and station distribution. However, the station corrections estimated in this study is based on the ak135 model. The application of direction-dependent traveltime corrections to seismic stations distributed across the region is expected to improve earthquake locations around the Sumatra Subduction Zone (SSZ) and its environs.

II.   Materials and Methods

2.1 The Study Region

The study region encompasses the Sumatra Fault System (SFS) which runs parallel to the SSZ (**Fig. 1**) where the Indo-Australia plate subducts beneath the Burma microplate and Sunda Block (Amalfi et al., 2016). The predominant tectonic structures in the area are the SSZ and the SFS. According to some authors (e.g., Irsyam et al., 2008; Lin et al., 2009) the SFS consist of 19 segments. The segments are separated by dilatational and contractional step-overs and abrupt changes in trend (Sieh and Natawidjaja, 2000). A total of 113 seismic stations recorded 100 or more earthquakes within the window of events used in this study. The seismic stations are distributed around the southern part of Thailand, Peninsular Malaysia, Singapore and the Island of Sumatra (Indonesia). The station distribution spans latitudes 10º N – 10º S and longitudes 93º E – 115º E (**Fig. 1**).

Figure 1. Distribution of seismic stations across the region.

2.2 Data

Earthquake data of magnitude ≥ 3.5 m_b used in this study spans latitudes 10° N $-$ 10° S and longitudes 93° E-115° E (**Fig. 2**) with maximum focal depth of 100 km. The earthquake epicenters (**Fig. 2**) are distributed over an area ~ 1,970,000 km^2 which is roughly the size of Mexico. The data is obtained from two sources: (1) the Incorporated Research Institutions for Seismology (IRIS) and (2) the Bulletin of International Seismological Center (ISC). A software (JWEED) developed by Seismology Department at the University of South Carolina (USC, 2012) is used to retrieve waveforms from the IRIS website for the period between the year 2006 and 2018. The reviewed ISC data is usually about 24 months behind time because arrival times are manually checked by ISC analysts (ISC, 2019). Picked phases from the IRIS waveforms are combined with the dataset from the ISC to obtain a total of 15,180 events. The combined dataset contains 97,124 p-wave first arrival times.
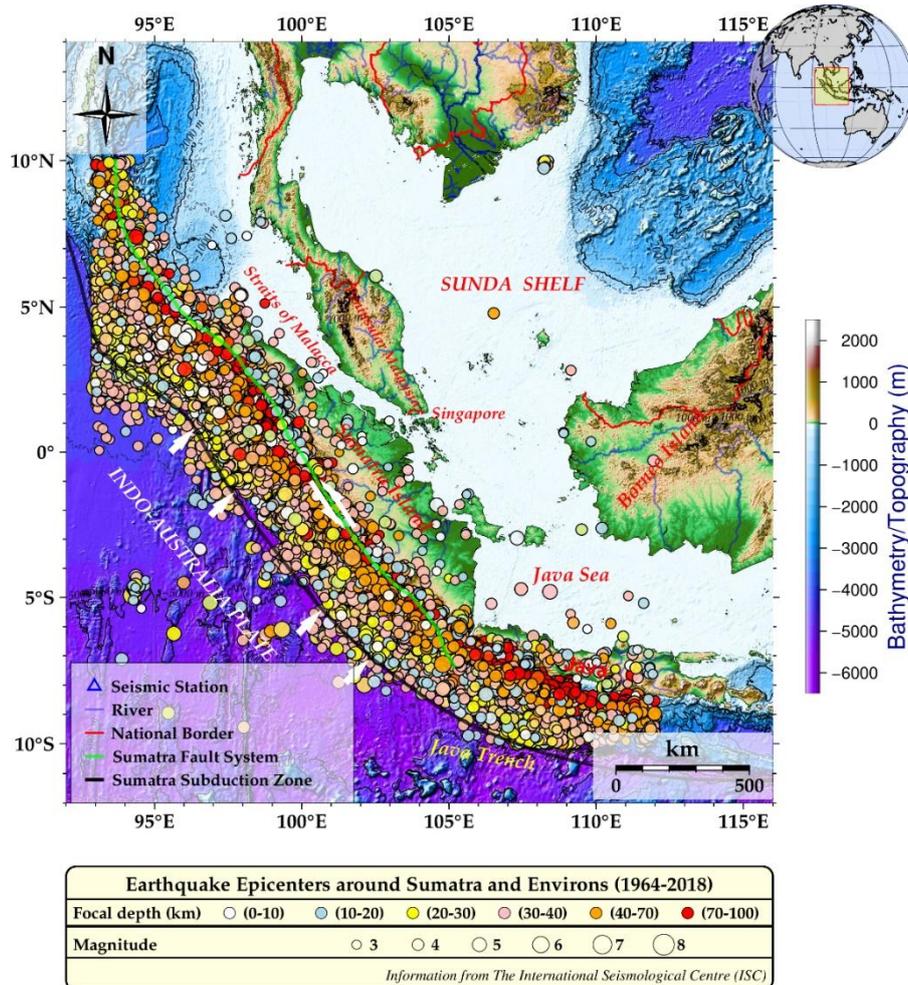
Figure 2. Earthquake epicenters across the region.

2.3 Methodology

Phase picking from the IRIS waveforms is done with the SEISAN software (Havskov and Ottemoller, 1999). The corresponding S-file from SEISAN is added to the ISC dataset. A new scheme (CONVT) developed in this study reads the combined file formats. The scheme operates within certain conditions which are predefined by the user (e.g., the limiting boundaries of the study area, the maximum depth of events, maximum epicentral distance and the residual limits). If the limiting boundaries of the study area are not set, CONVT will extract the limits from the largest and smallest values of latitudes and longitudes of the station distribution. Both the ISC dataset and the IRIS summary file formats can be converted into S-file format for use by the SEISAN software. Since waveforms can be registered into SEISAN database, this conversion will be useful in validating arrival times from other sources. The routine extracts the number of stations with arrival time data and the combined dataset is converted to a format as an input file for the next stage.

This study introduces a ray tracing algorithm (TRAVT) to compute raypaths and traveltimes in 3D. The hypocentral parameters reported by both the ISC and the IRIS are used in this study. Firstly, TRAVT initiate the station coordinates, the selected 1D velocity model, and the dataset. Then, a 3D grid model is constructed from the selected 1D velocity model using the parameterization technique introduced by Zhao *et al.* (1992). This parameterization technique has been used for tomographic studies (e.g., Wang et al., 2017). Using the haversine formula, TRAVT calculates the epicentral distance, the hypocentral distance and the azimuth. A subroutine (TRAYD) that uses a technique introduced by Kim and Baag (2002) calculates the take-off angle for up-going rays from the source (**Fig. 3**). This two-point ray shooting technique has been used by some authors (e.g., Osagie and Kim, 2013; Osagie, et al., 2017). Another subroutine (TRAYR) computes raypaths and traveltimes for refracted rays from all existing boundaries in the model. The ray with the shortest traveltime from the result of TRAYD and TRAYR is selected and the wave type is determined within TRAVT.
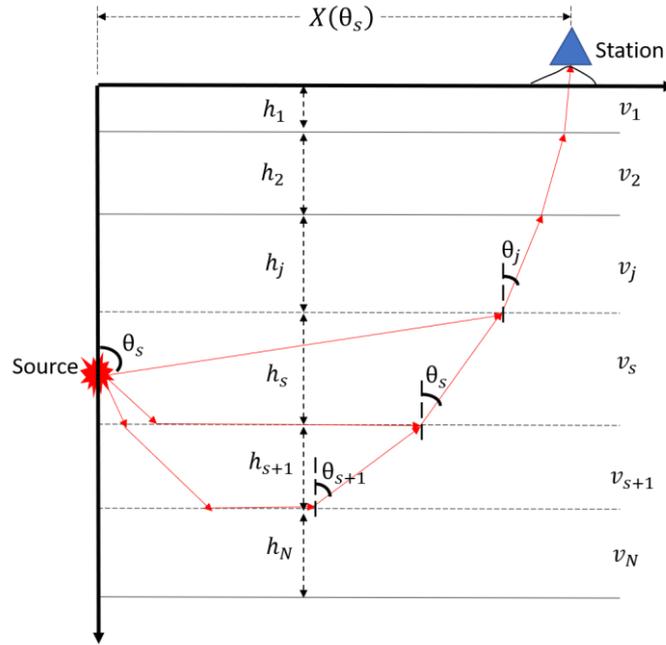
Figure 3 A schematic diagram showing ray-paths (red arrow lines) for both direct and refracted rays in an N-layered model with the thicknesses h_j and velocities v_j. The source is at the layer with thickness h_s and velocity v_s and the station (blue triangle at some elevation).

The computed rays are constrained to bottom in each layer between interfaces and might be reflected off the top of the layer or turn within the layer to retain raypath with the shortest traveltime. Apart from boundary values, the various points are determined by a predefined value of step-length as the rays propagate from source to stations. A variable is defined that carries information (latitude, longitude, depth, velocity, time from source, raypath length from source, angle ray makes the vertical) at various points along the path step-length between source and station. The depth of refraction for any boundary are adjustable within the scheme. TRAVT has the advantage of rapid convergence resulting in less computational time and resources. The scheme can accommodate a model with as many layers as required for computing traveltimes for local and regional investigation of the sub-surface. This can be useful for both field seismic investigations, generation of synthetic seismograms, determination of refraction depths and to estimate crustal thicknesses/Moho depths. It can also be used for the forward calculation process of tomographic inversions and has been successfully integrated into a tomographic scheme. The flowchart (**Fig. 4**) shows the process from data collection, preparation, analysis and computation.
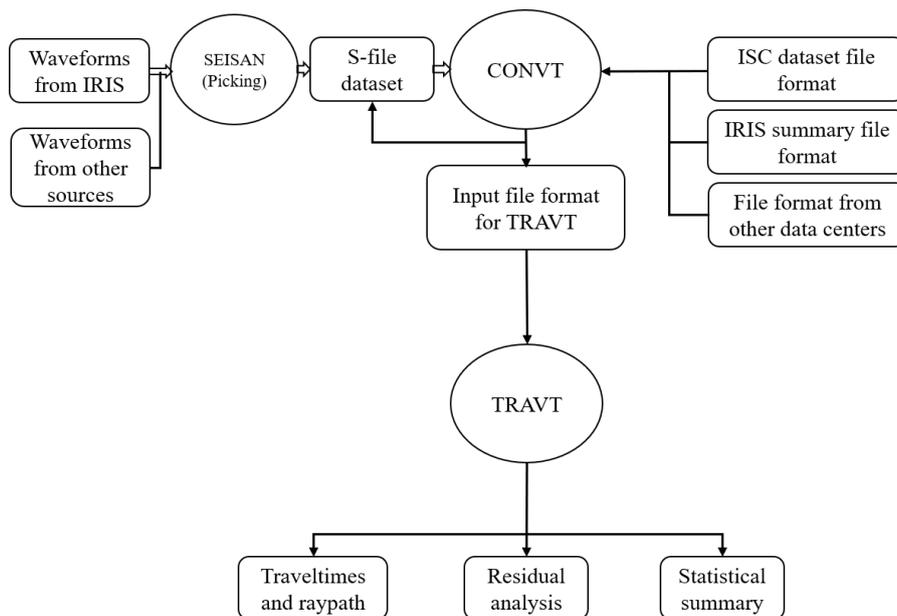
Figure 4   Flowchart of data collection, analysis and computation (circles are the algorithms)

III. Results and Discussion

The traveltime result of manual picks from the IRIS waveforms are validated by the TauP Toolkit software for the same velocity model, hypocenters and station distribution around the study area. Figure 5 shows raypaths for P_g and P_n phases from events to stations (note that the depth axis is about 50 times exaggerated). Traveltime residuals are compared with the result published by the ISC for the same "Event ID" and "Arrival ID" (**Table 1**). The table shows the average traveltime residual (**AR**) computed with respect to back-azimuth (θ) within four quadrants: NE ($\theta \leq 90°$), SE ($90° < \theta \leq 180°$), SW ($180° < \theta \leq 270°$) and NW ($270° < \theta \leq 360°$). The total number of arrivals recorded by the stations range from 100 to 5425 for stations SBSI (in indonesia) and KULM (in Malaysia), respectively. Columns $12 - 15$ show the average traveltime residual values (**AR**) estimated at the four θ ranges for each station. Columns 16 and 17 are the average A**R** calculated over all directions and from the ISC results, respectively.
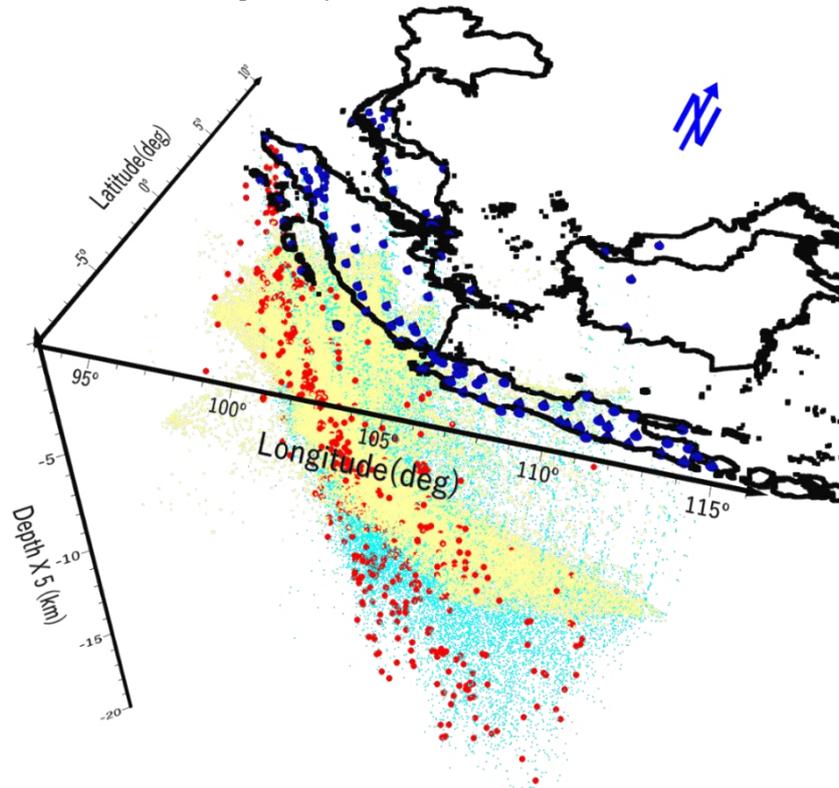
Figure 5 Points along raypaths for P_g (cyan) and P_n (yellow) phases calculated using the ak135 model (depth axis is 55 times exaggerated)

Table 1 Calculated average residual (AR) at four back-azimuthal directions (columns 12-15). Columns 16 and 17 are the overall calculated (AR) and ISC (AR).

Sn	Station Code	Latitude (deg)	Longitude (deg)	Elevation (km)	Country	No. of Arrivals	θ≤90°	90°<θ ≤180°	180°<θ ≤270°	270°<θ ≤360°	θ≤90°	90°<θ ≤180°	180°<θ ≤270°	270°<θ ≤360°	AR -Cal	AR-ISC
								Number of Arrivals				Average Traveltime Residual (seconds)				
1	SBSI	1.5500	98.8900	0.1470	Indonesia	100	9	29	62	0	0.96	-1.23	0.86	0.00	0.26	0.11
2	CLJI	-7.7187	109.0150	0.0460	Indonesia	114	0	17	64	33	0.00	-0.40	0.46	0.73	0.41	0.11
3	EGSI	-5.3526	102.2767	0.0360	Indonesia	115	9	38	2	66	0.22	0.51	0.35	-0.30	0.02	-0.19
4	STKI	0.0656	111.4772	0.0880	Indonesia	117	0	2	109	6	0.00	1.44	1.17	0.38	1.13	1.28
5	SIMI	2.6889	98.9469	1.6810	Indonesia	119	0	45	41	33	0.00	-0.05	0.91	1.10	0.60	0.37
6	TRSI	2.0256	98.9594	0.9790	Indonesia	121	0	39	49	33	0.00	0.64	0.36	0.72	0.55	0.49
7	DJA	-6.1833	106.8362	0.0080	Indonesia	137	0	21	46	70	0.00	1.06	0.57	0.77	0.75	0.44
8	MED	3.5500	98.6833	0.0320	Indonesia	137	0	53	39	45	0.00	0.45	0.69	0.50	0.53	0.39
9	RBSI	-5.8445	105.7420	0.0000	Indonesia	142	0	33	44	65	0.00	0.53	-0.29	1.00	0.49	0.32
10	PBKI	-2.7047	111.6697	0.0740	Indonesia	145	0	4	130	11	0.00	0.64	1.02	0.38	0.96	0.94
11	SEMI	2.4603	98.3917	1.7500	Indonesia	153	2	73	26	52	0.07	-0.53	0.42	0.59	0.02	-0.12
12	TBJI	-6.8179	111.8481	0.0000	Indonesia	166	0	4	136	26	0.00	1.04	1.02	0.85	0.99	0.76
13	KRKI	-8.1583	112.4525	0.0000	Indonesia	178	0	0	100	78	0.00	0.00	0.68	0.91	0.78	0.51
14	PCBI	1.8900	98.9253	1.0000	Indonesia	180	2	66	41	71	0.23	-0.42	0.48	0.51	0.16	0.04
15	UWJI	-6.4191	110.9474	0.0620	Indonesia	200	0	23	142	35	0.00	0.96	0.92	1.17	0.97	0.78
16	KELI	-8.2167	114.4910	0.5910	Indonesia	202	0	0	52	150	0.00	0.00	2.35	1.93	2.04	0.61
17	AEKI	2.1017	98.4536	0.8400	Indonesia	223	0	117	29	77	0.00	0.16	0.12	0.55	0.29	-0.49
18	SIBI	3.2408	98.5044	2.0500	Indonesia	224	0	106	59	59	0.00	1.03	1.41	1.39	1.23	0.34
19	BLJI	-7.7450	113.5950	0.0000	Indonesia	243	0	0	159	84	0.00	0.00	1.29	1.27	1.29	1.01
20	NGJI	-7.3676	111.4612	0.0000	Indonesia	245	1	20	143	81	1.96	1.19	1.50	1.23	1.39	1.07
21	MRPI	1.6125	99.3172	1.1000	Indonesia	246	1	152	41	52	0.44	1.01	0.72	1.29	1.01	-0.08
22	PACI	-6.5928	106.9100	0.8500	Indonesia	253	1	67	55	130	2.46	1.19	0.78	1.18	1.10	0.65
23	KMMI	-7.0500	113.9667	0.0000	Indonesia	261	0	0	136	125	0.00	0.00	0.46	0.88	0.66	0.44
24	ABJI	-7.7957	114.2342	0.0000	Indonesia	273	0	0	161	112	0.00	0.00	1.47	1.37	1.43	1.16
25	JCJI	-6.4900	108.2700	0.0000	Indonesia	278	2	59	147	70	1.22	-0.78	-0.30	1.43	0.05	-0.19
26	SINI	-7.0144	107.5000	1.0000	Indonesia	280	3	66	42	169	-1.24	0.93	0.57	0.92	0.85	0.39
27	GRJI	-6.9145	112.4793	0.0000	Indonesia	304	0	0	248	56	0.00	0.00	1.08	1.60	1.17	0.89
28	RANI	-8.4525	114.9490	0.5000	Indonesia	319	0	0	60	259	0.00	0.00	1.79	1.21	1.32	0.10
29	LARI	2.8856	98.1572	0.8200	Indonesia	322	0	175	59	88	0.00	0.25	0.36	1.23	0.54	-0.41
30	PULI	-6.3450	105.9760	1.3460	Indonesia	326	2	51	38	235	1.77	0.92	0.25	1.54	1.29	0.45

Table 1 Continues…

Sn	Station Code	Latitude (deg)	Longitude (deg)	Elevation (km)	Country	No. of Arrivals	θ≤90°	90°<θ ≤180°	180°<θ ≤270°	270°<θ ≤360°	θ≤90°	90°<θ ≤180°	180°<θ ≤270°	270°<θ ≤360°	AR -Cal	AR-ISC
								Number of Arrivals				Average Traveltime Residual (seconds)				
31	PASI	-6.6894	105.5890	0.2200	Indonesia	351	2	109	29	211	1.28	0.47	-0.32	0.48	0.41	-0.35
32	YOGI	-7.8166	110.2949	0.1600	Indonesia	363	10	87	171	95	0.85	0.12	0.17	0.50	0.26	0.03
33	KALI	-7.1064	106.6590	0.8100	Indonesia	393	10	39	19	325	0.15	0.54	0.07	0.83	0.75	-0.40
34	CBJI	-6.4200	106.8500	0.0000	Indonesia	399	2	43	194	160	0.84	-0.73	0.58	1.88	0.96	0.53
35	TRT	-7.7040	112.6350	0.0000	Indonesia	405	0	0	161	244	0.00	0.00	0.89	1.02	0.97	0.51
36	WOJI	-7.8372	110.9236	0.0000	Indonesia	405	3	36	229	137	-0.09	0.26	0.34	0.79	0.49	0.20
37	BJII	-7.3329	109.7096	0.6290	Indonesia	412	1	33	226	152	-1.03	0.65	0.40	0.69	0.52	0.42
38	JMBI	-1.6335	103.6417	0.0000	Indonesia	412	1	32	301	78	3.39	1.08	0.92	0.72	0.90	0.77
39	TPRI	0.9184	104.5263	0.0410	Indonesia	422	0	27	291	104	0.00	0.70	0.77	0.85	0.78	0.71
40	GMJI	-8.2732	113.4441	0.0000	Indonesia	479	0	0	213	266	0.00	0.00	0.90	1.11	1.02	0.72
41	SRDI	-8.4794	114.1420	0.2900	Indonesia	497	0	0	97	400	0.00	0.00	1.11	1.21	1.19	-0.16
42	SJI	-7.7349	111.7669	0.7230	Indonesia	529	1	4	222	302	1.12	0.33	0.76	0.53	0.62	0.30
43	PMBI	-2.9270	104.7720	0.0300	Indonesia	560	3	72	367	118	0.03	0.79	0.42	0.04	0.39	0.27
44	PENI	-5.5667	105.1710	0.2000	Indonesia	587	3	140	128	316	-0.48	0.91	1.16	1.67	1.37	0.47
45	KPJI	-7.3330	108.9310	0.0000	Indonesia	645	6	114	272	253	1.22	1.20	1.04	1.06	1.08	0.76
46	TNG	-6.1717	106.6462	0.0140	Indonesia	647	1	142	251	253	0.15	1.18	0.86	0.91	0.95	0.56
47	RGRI	-0.3491	102.3338	0.0410	Indonesia	650	0	71	466	113	0.00	0.88	0.82	0.71	0.81	0.68
48	TPI	-2.7563	107.6534	0.0250	Indonesia	654	2	70	409	173	-0.29	1.14	0.78	0.86	0.83	0.71
49	PBSI	-0.0547	98.2800	0.0000	Indonesia	728	62	249	30	387	0.66	0.15	0.14	0.52	0.39	0.08
50	PPBI	-2.1616	106.1364	0.0640	Indonesia	744	2	112	511	119	-1.14	1.14	0.91	1.06	0.96	0.87
51	RPSI	2.6951	98.9240	0.0000	Indonesia	746	1	155	262	328	-1.35	-0.53	0.71	0.87	0.52	0.34
52	KRJI	-2.0912	101.4619	0.8110	Indonesia	753	1	213	227	312	1.16	0.72	0.38	0.82	0.66	0.46
53	SBJI	-6.1200	106.1300	0.0000	Indonesia	754	2	245	253	254	0.25	0.99	0.33	0.73	0.68	0.39
54	BLSI	-5.3676	105.2452	0.1470	Indonesia	764	1	199	310	254	1.99	0.70	0.57	1.07	0.77	0.48
55	KLSI	-4.6900	104.7300	0.0810	Indonesia	804	1	159	227	417	-1.53	0.92	0.81	0.62	0.73	0.53
56	SMRI	-7.0491	110.4407	0.2030	Indonesia	817	4	111	459	243	0.20	1.06	1.20	0.90	1.08	0.83
57	SNSI	2.4089	96.3267	0.0140	Indonesia	821	54	417	64	286	1.33	0.25	0.12	0.24	0.31	-0.04
58	PCJI	-8.1947	111.1771	0.0000	Indonesia	844	6	59	297	482	0.02	-0.47	0.51	0.46	0.34	0.07
59	CMJI	-7.7837	108.4485	0.0000	Indonesia	853	7	173	208	465	-0.08	0.15	-0.05	0.01	0.02	-0.25
60	MLSI	4.2668	96.4040	0.0580	Indonesia	869	18	402	264	185	-0.26	-0.01	0.32	0.37	0.17	-0.04

Table 1 Continues…

Sn	Station Code	Latitude (deg)	Longitude (deg)	Elevation (km)	Country	No. of Arrivals	θ≤90°	90°<θ ≤180°	180°<θ ≤270°	270°<θ ≤360°	θ≤90°	90°<θ ≤180°	180°<θ ≤270°	270°<θ ≤360°	AR -Cal	AR-ISC
								Number of Arrivals				Average Traveltime Residual (seconds)				
61	DBJI	-6.5538	106.7497	0.2110	Indonesia	898	3	235	229	431	0.31	1.05	0.60	0.61	0.72	0.45
62	BSI	5.4964	95.2961	0.1920	Indonesia	902	1	705	117	79	-1.17	-0.69	-0.09	0.11	-0.55	-0.57
63	SKJI	-7.0053	106.5563	0.1000	Indonesia	924	7	361	168	388	0.60	0.59	-0.07	0.46	0.41	0.10
64	CNJI	-7.3090	107.1296	0.0000	Indonesia	959	7	326	157	469	-0.02	0.40	-0.08	-0.26	0.00	-0.28
65	LHSI	-3.8267	103.5233	0.0000	Indonesia	999	3	185	335	476	-1.08	1.20	0.86	0.84	0.90	0.71
66	PWJI	-8.0220	111.8039	0.0000	Indonesia	999	1	6	480	512	0.35	0.01	0.46	0.58	0.52	0.23
67	JAGI	-8.4702	114.1521	0.1710	Indonesia	1014	0	0	338	676	0.00	0.00	0.72	0.61	0.65	0.38
68	MASI	-3.1415	102.2396	0.3840	Indonesia	1058	6	312	264	476	0.39	0.90	0.42	0.71	0.69	0.46
69	KLI	-4.8630	104.8567	0.0320	Indonesia	1096	3	256	364	473	1.06	1.07	0.86	0.82	0.89	0.65
70	SDSI	-0.9324	101.4282	0.0000	Indonesia	1127	0	207	554	366	0.00	0.52	0.56	0.84	0.64	0.35
71	CGJI	-6.6135	105.6929	0.0000	Indonesia	1212	1	395	123	693	-1.26	0.46	-0.14	-0.24	0.00	-0.24
72	PPSI	-2.7630	100.0096	0.0000	Indonesia	1276	119	565	154	438	0.37	0.29	-0.63	0.14	0.14	-0.04
73	KCSI	3.5220	97.7715	0.2050	Indonesia	1374	1	433	683	257	0.97	0.07	0.59	1.18	0.54	0.17
74	TPTI	3.2600	97.1800	0.0090	Indonesia	1375	7	484	596	288	0.33	0.00	-0.33	0.35	-0.07	-0.30
75	TSI	3.5008	98.5645	0.0000	Indonesia	1418	1	322	785	310	-0.19	0.33	0.99	1.03	0.85	0.58
76	SISI	-1.3265	99.0895	0.0000	Indonesia	1524	72	792	32	628	0.67	-0.17	0.17	0.29	0.07	-0.11
77	CISI	-7.5557	107.8153	0.5440	Indonesia	1541	10	336	269	926	0.67	0.22	-0.22	-0.41	-0.23	-0.48
78	UGM	-7.9125	110.5231	0.3500	Indonesia	1553	13	127	541	872	0.69	0.40	0.15	0.43	0.33	0.08
79	LHMI	5.2288	96.9472	0.0030	Indonesia	1623	5	491	805	322	0.56	0.06	0.58	0.57	0.42	0.24
80	KSI	-3.6517	102.5929	0.5390	Indonesia	1686	3	555	354	774	0.25	0.38	0.16	0.44	0.36	0.22
81	BKNI	0.3262	101.0396	0.0650	Indonesia	1723	3	316	692	712	-0.11	0.14	0.61	0.67	0.55	0.37
82	LWLI	-5.0175	104.0589	0.9380	Indonesia	1767	7	408	372	980	0.87	0.98	0.24	0.51	0.57	0.37
83	PDSI	-0.9118	100.4617	0.2760	Indonesia	1804	9	578	542	675	0.18	-0.12	-0.29	0.44	0.04	-0.12
84	KASI	-5.5236	104.4967	0.0000	Indonesia	1921	5	497	327	1092	0.22	0.67	-0.24	0.16	0.22	0.02
85	MNSI	0.7955	99.5796	0.0000	Indonesia	1956	0	571	381	1004	0.00	-0.02	0.21	0.76	0.43	0.21
86	MDSI	-4.4861	104.1783	0.0000	Indonesia	2053	2	444	468	1139	-0.63	0.90	0.54	0.25	0.45	0.28
87	LEM	-6.8266	107.6175	1.2930	Indonesia	2173	8	472	560	1133	1.13	1.13	1.01	1.00	1.03	0.80
88	PPI	-0.4568	100.3970	0.0000	Indonesia	2403	2	843	680	878	1.22	0.20	0.11	0.61	0.32	0.13
89	MNAI	-4.3605	102.9557	0.1540	Indonesia	2538	13	723	398	1404	0.15	0.63	0.14	0.20	0.31	0.16
90	GSI	1.3039	97.5755	0.1070	Indonesia	2866	140	1224	365	1137	0.63	-0.32	0.11	0.34	0.05	-0.17

Table 1 Continues…

Sn	Station Code	Latitude (deg)	Longitude (deg)	Elevation (km)	Country	No. of Arrivals	θ≤90°	90°<θ ≤180°	180°<θ ≤270°	270°<θ ≤360°	θ≤90°	90°<θ ≤180°	180°<θ ≤270°	270°<θ ≤360°	AR -Cal	AR-ISC
								Number of Arrivals				Average Traveltime Residual (seconds)				
91	PSI	2.8010	98.9240	0.9870	Indonesia	5334	6	1410	2489	1429	0.68	-0.93	0.02	1.09	0.06	-0.11
92	KLM	3.1025	101.6450	0.0460	Malaysia	175	0	23	98	54	0.00	1.23	1.43	0.43	1.09	0.73
93	SBUM	2.4500	112.2200	0.0310	Malaysia	331	0	0	328	3	0.00	0.00	0.48	0.72	0.48	0.83
94	DSRI	-0.4793	104.5778	0.0580	Malaysia	551	1	58	388	104	-1.41	1.00	0.76	0.77	0.78	0.72
95	KTGM	5.3280	103.1340	0.0560	Malaysia	656	0	12	619	25	0.00	-0.14	0.51	0.77	0.51	0.64
96	FRIM	3.2370	101.6250	0.0980	Malaysia	711	0	55	565	91	0.00	0.30	0.65	0.08	0.55	0.55
97	KSM	1.4733	110.3083	0.0660	Malaysia	876	0	22	782	72	0.00	-0.06	0.54	0.99	0.56	0.45
98	KGM	2.0157	103.3190	0.1030	Malaysia	1675	3	128	1085	459	1.70	0.53	1.19	1.03	1.09	0.69
99	MYKOM	1.7900	103.8500	0.0000	Malaysia	2152	0	121	1347	684	0.00	0.01	0.63	0.34	0.51	0.40
100	IPM	4.4795	101.0255	0.2470	Malaysia	3790	5	380	2671	734	0.72	0.42	0.89	0.20	0.71	0.37
101	KULM	5.2900	100.6500	0.0740	Malaysia	5425	5	452	4501	467	1.78	-0.41	0.91	0.69	0.78	-0.03
102	KAPK	1.2967	103.8823	-0.0290	Singapore	140	2	0	61	77	0.45	0.00	0.74	0.39	0.54	0.00
103	BESC	1.3422	103.8513	0.0030	Singapore	262	2	0	111	149	0.43	0.00	0.63	0.25	0.41	0.00
104	NTU	1.3537	103.6852	0.0050	Singapore	311	0	0	132	179	0.00	0.00	0.68	0.13	0.37	0.00
105	BTDF	1.3608	103.7729	0.0640	Singapore	575	2	10	336	227	0.16	0.15	0.59	0.23	0.44	0.18
106	KRAB	8.2215	99.1965	0.0580	Thailand	115	1	16	97	1	-0.17	-0.08	0.56	0.87	0.47	0.60
107	SURT	8.9577	98.7950	0.0260	Thailand	182	1	8	168	5	-0.39	-0.33	0.46	1.06	0.44	0.50
108	SURA	9.1663	99.6295	-0.0050	Thailand	183	0	22	161	0	0.00	-0.22	0.23	0.00	0.18	0.20
109	PKDT	7.8920	98.3350	0.0530	Thailand	248	1	20	219	8	-2.15	0.45	0.30	1.03	0.32	0.26
110	TRTT	7.8362	99.6912	0.0710	Thailand	333	1	35	286	11	-0.14	-0.72	0.05	0.46	-0.02	0.03
111	SRIT	8.5955	99.6020	0.0580	Thailand	358	0	46	306	6	0.00	-0.70	0.26	0.23	0.13	0.06
112	SKLT	7.1700	100.6200	0.0140	Thailand	436	1	31	392	12	-0.21	-0.70	0.43	0.34	0.34	0.29
113	SNG	7.1770	100.6170	0.0040	Thailand	1100	3	154	835	108	0.37	-0.51	0.94	1.19	0.76	0.09

IV. Conclusion

This study introduces an algorithm for use in local and regional seismic ray tracing in 1D/3D models. The algorithm can accommodate any model with as many layers to compute local/regional raypaths and traveltimes in sub-surface investigations. The algorithm has been incorporated successfully for forward calculations in a scheme for 3D tomographic studies. The algorithm will be useful for other applications like generating synthetic seismograms. A total of 113 broadband stations distributed around the southern part of Thailand, Peninsular Malaysia, Singapore and the Island of Sumatra in Indonesia recorded 100 or more earthquakes within the window of the selected events. The average residual values at the four back-azimuthal directions (NE, SE, SW and NW) show varying degrees of heterogeneities. The average residual values over all angles from the seismic station range from -0.02 to 0.76 seconds (s) for the 8 seismic stations in southern Thailand which are selected in this study. Positive average residual values (between 0.48 s and 1.09 s) are estimated for 10 seismic stations within Peninsular Malaysia. The average residual values for the 4 seismic stations in Singapore range between 0.37 s and 0.54 s. For the 91 seismic stations which are distributed around

the Sumatra region of Indonesia, average residual values range from -0.07 s to 2.04 s. The result of this study will support routine location of hypocentral parameters within the region.

Acknowledgement

References

[1]. Amalfi, O., Phil, C., David, R., and Sri, H. (2016). Sensitivity analysis for probabilistic seismic hazard analysis (PSHA) in the Aceh Fault Segment, Indonesia. *Geological Society, London, Special Publications, 441*, 121-131. doi: https://doi.org/10.1144/SP441.5

[2]. Crotwell, H. P., Owens, T. J., and Ritsema, J. (1999). The TauP Toolkit: Flexible seismic travel-time and ray-path utilities. *Seismological Research Letters, 70*(2), 154-160.

[3]. Dziewonski, A. M., and Anderson, D. L. (1981). Preliminary reference Earth model. *25*(4), 297-356.

[4]. Havskov, J., and Ottemoller, L. (1999). SEISAN earthquake analysis software. *Seismological Research Letters, 70*(5), 532-534.

[5]. Irsyam, M., Dangkua, D. T., Hoedajanto, D., Hutapea, B. M., Kertapati, E. K., Boen, T., and Petersen, M. D. (2008). Proposed seismic hazard maps of Sumatra and Java islands and microzonation study of Jakarta city, Indonesia. *Journal of earth system science, 117*(2), 865-878.

[6]. ISC. (2019). International Seismological Center Bulletin. Retrieved from http://www.isc.ac.uk/

[7]. Kang, Y.-A., Kim, W., and Kang, T.-S. (2013). Relocation of earthquakes beneath the East Sea of Korea: uncertainty of hypocentral parameters caused by refracted waves. *Geosciences Journal, 17*(2), 173-182.

[8]. Kennett, B., and Engdahl, E. (1991). Traveltimes for global earthquake location and phase identification. *Geophysical Journal International, 105*(2), 429-465.

[9]. Kennett, B. L., Engdahl, E. R., and Buland, R. (1995). Constraints on seismic velocities in the Earth from traveltimes. *eophysical Journal International, 122*(1), 108-124.

[10]. Kim, W., and Baag, C.-E. (2002). Rapid and accurate two-point ray tracing based on a quadratic equation of takeoff angle in layered media with constant or linearly varying velocity functions. *Bull. Seism. Soc. Am, 92*(6), 2251-2263.

[11]. Lin, J.-Y., LePichon, X., Claude, R., Jean-Claude, S., and Tanguy, M. (2009). Spatial aftershock distribution of the 26 December 2004 great Sumatra-Andaman earthquake in the northern Sumatra area. *Geochem Geophys Geosyst, 10*(2009), 1-15. doi:doi:10.1029/2009GC002454

[12]. Osagie, A., Nawawi, M., Khalil, A. E., and Abdullah, K. (2017). Regional travel-time residual studies and station correction from 1-D velocity models for some stations around Peninsular Malaysia and Singapore. *NRIAG Journal of Astronomy Geophysics, 6*(1), 19-29.

[13]. Osagie, A. U., and Kim, W. (2013). Relocation of Earthquakes that Occurred Beneath Parkfield Region of California using VELHYPO. *IOSR Journal of Applied Geology and Geophysics, 1*(3), 66-81.

[14]. Shearer, P. M. (2001). Improving Global Seismic Event Locations Using Source-Receiver Reciprocity. *Bulletin of the Seismological Society of America, 91*, 594–603.

[15]. Sieh, K., and Natawidjaja, D. (2000). Neotectonics of the Sumatran fault, Indonesia. *Journal of Geophysical Research, 105*(B12), 28295-28326.

[16]. Spakman, W., and Bijwaard, H. (2001). Optimization of cell parameterizations for tomographic inverse problems. In *Monitoring the Comprehensive Nuclear-Test-Ban Treaty: Surface Waves* (pp. 1401-1423): Springer.

[17]. USC. (2012). JWEED. South Carolina Seismology Department at the University of South Carolina. Retrieved from http://www.seis.sc.edu/software

[18]. Villaseñor, A., Barmin, M. P., Ritzwoller, M. H., and Levshin, A. L. (2003). Computation of regional travel times and station corrections from three-dimensional velocity models. *Stud. Geophys. Geod.*

[19]. Wang, Z., Zhao, D., Liu, X., Chen, C., and Li, X. (2017). P and S wave attenuation tomography of the Japan subduction zone. *Geochemistry, Geophysics, Geosystems, 18*(4), 1688-1710.

[20]. Wessel, P., Luis, J. F., Uieda, L., Scharroo, R., Wobbe, F., Smith, W. H. F., and Tian, D. (2019). The generic mapping tools version 6. *Geochemistry, Geophysics, Geosystems*.

[21]. Yang, X., Bondár, I., McLaughlin, K., and North, R. (2001). Source specific station corrections for regional phases at Fennoscandian stations. *Pure and Applied Geophysics*, 35-57.

[22]. Zhao, D., Hasegawa, A., and Horiuchi, S. (1992). Tomographic imaging of P and S wave velocity structure beneath northeastern Japan. *Journal of Geophysical Research, 97*(B13), 19909-19928.

[23]. Zhao, D., and Lei, J. (2004). Seismic ray path variations in a 3D global velocity model. *Physics of the Earth Planetary Interiors, 141*(3), 153-166.